MCP Papers in Press. Published on June 19, 2012 as Manuscript M112.019315

Bacterial Responses to a Simulated Colon Tumor Microenvironment

Annemarie Boleij[1], Bas E. Dutilh[2,3], Guus Kortman[1], Rian Roelofs[1],Coby M. Laarakkers[1], Udo F. Engelke[1] and Harold Tjalsma[1*]

[1]Department of Laboratory Medicine/ 830, Radboud University Medical Centre, P.O. Box 9101, 6500 HB Nijmegen, the Netherlands, Nijmegen Institute for Infection, Inflammation and Immunity (N4i) & Radboud University Centre for Oncology (RUCO), [2]Centre for Molecular and Biomolecular Informatics, Nijmegen Centre for Molecular Life Sciences, Radboud University Medical Centre, Geert Grooteplein 28, 6525 GA Nijmegen, the Netherlands and [3]Departments of Computer Science and Biology, San Diego State University, 5500 Campanile Drive, San Diego CA 92182, United States of America.

***Corresponding author:** Mailing address: Department of Laboratory Medicine / 830, Radboud University Medical Centre, P.O. Box 9101, 6500 HB Nijmegen, the Netherlands. Phone: +31-24-3618947. Fax: +31-24-3668754. E-mail: H.Tjalsma@labgk.umcn.nl

Running title: *Streptococcus gallolyticus* forages on tumor cell metabolites

Key words: metabolites / colorectal cancer / *Streptococcus gallolyticus* / microenvironment / gut microbiome

ABBREVIATIONS

BHI, brain heart infusion broth

CRC, colorectal cancer

DMEM, Dulbecco's modified Eagle's medium

FC, fold change

FCS, fetal calf serum

FDR, false discovery rate

F6P, fructose 6-phosphate

G13P, glycerate-1,3-phosphate

G6P, glucose-6-phosphate

MRS, Man, Rogosa and Sharpe broth

OD, optical density

PCA, principal component analyses

3PG, 3-phosphate glyceric acid

SUMMARY

One of the few bacteria that have been consistently linked to colorectal cancer (CRC) is the opportunistic pathogen *Streptococcus gallolyticus*. *S. gallolyticus* infections are generally regarded as an indicator for colonic malignancy, while the carriage rate of this bacterium in the healthy large intestine is relatively low. We speculated that the physiological changes accompanying the development of CRC might favor the colonization of this bacterium. To investigate whether colon tumor cells can support the survival of *S. gallolyticus*, *S. gallolyticus* was grown in spent medium of malignant colonocytes to simulate the altered metabolic conditions in the CRC microenvironment. These *in vitro* simulations indicated that *S. gallolyticus* had a significant growth advantage in these spent media, which was not observed for other intestinal bacteria. Under these conditions, bacterial responses were profiled by proteome analysis and metabolic shifts were analyzed by ^{1}H-NMR-spectroscopy. *In silico* pathway analysis of the differentially expressed proteins and metabolite analysis indicated that this advantage resulted from the increased utilization of glucose, glucose derivates and alanine. Together, these data suggest that tumor cell metabolites facilitate the survival of *S. gallolyticus,* favoring its local outgrowth and providing a possible explanation for the specific association of *S. gallolyticus* with colonic malignancy.

INTRODUCTION

The human intestine is the habitat for several hundred different bacterial species with an increasing bacterial concentration and variability towards the distal colon (1). The resident gut microbiota is essential for human health by making dietary nutrients available to the host and preventing the invasion of pathogens by competitive colonization and nutrient competition (2, 3). Strikingly, the part of the intestine with the highest bacterial colonization, the colon, is also most affected by cancer, with 146,970 annual cases in the United States of America (4). In a healthy colonic environment, the host has several defense mechanisms to shield itself from bacterial infection, such as the viscous mucus layer overlaying the epithelium. However, the progression of CRC is accompanied by changes in the integrity of the colon, including reduced mucus production (5) and increased epithelial permeability (6). These physiological changes can drive the intestinal ecosystem, which is relatively stable during adult life, into dysbiosis (7, 8). As a consequence, the host may become more susceptible to opportunistic bacterial infections (9-11).

One of the few bacteria that have been consistently linked to CRC is the opportunistic pathogen *Streptococcus gallolyticus* (previously known as *Streptococcus bovis* biotype I). In CRC patients the fecal carriage rate of this bacterium is increased from 10% to about 50% (12), which suggests that this disease facilitates the colonic survival of *S. gallolyticus*. Importantly, approximately 60% of patients that present with *S. gallolyticus* endocarditis have concomitant CRC (both adenomas and carcinomas)(13) (14), which largely exceeds the rates reported in the general population (~25%) (15). These patients had no gastro-intestinal signs or clinical symptoms of malignancy and CRC was only detected because this bacterial infection guided the physician to perform a colonoscopy.

Several mechanisms for this apparent association between *S. gallolyticus* and CRC can be envisaged. Recently, we postulated a model in which the collagen binding ability of *S. gallolyticus* contributes to the specific colonization of malignant colonic sites (16). However, the altered microenvironment of the tumor may also provide conditions that favor survival

and outgrowth of *S. gallolyticus* in this newly formed intestinal niche. For example, Hirayama *et a*l. have shown that glucose-1-phosphate and fructose-1-phophate levels as well as amino acid concentrations were significantly higher in tumor tissue than in normal tissue (17). To investigate if this altered nutritional status of the CRC microenvironment could facilitate the foraging of *S. gallolyticus*, we simulated the influence of colon tumor cell metabolites on *S. gallolyticus* growth by incubating this bacterium in spent medium of malignant cells. Subsequently, the bacterial responses were profiled by two-dimensional proteome analysis, and metabolic shifts in the culture medium were assessed by ^{1}H-NMR-spectroscopy. *In silico* pathway analysis and further *in vitro* simulations showed that, unlike other intestinal bacteria, *S. gallolyticus* had a growth advantage under these conditions, which could mainly be attributed to increased glycolysis. These results provide the first molecular support that tumor metabolites may facilitate the local outgrowth of tumor-foraging bacteria, such as *S. gallolyticus*.

EXPERIMENTAL PROCEDURES

Cell culture and bacterial strains - Colorectal adenocarcinoma cell lines HT-29, SW480, HCT116 and Caco-2 (www.atcc.org) were cultured in Dulbecco's Modified Eagle's Medium (DMEM, Lonza) supplemented with 10% Fetal Calf Serum (FCS) (further indicated as standard medium) at 37°C/5% CO_2. These culturing conditions were used unless stated otherwise. The following bacterial strains were used; *Enterococcus faecalis* 19433 (www.atcc.org), *Lactobacillus plantarum* WCFS1 (18) and *E. coli Nissle* 1917 (obtained from Julian Marchesi).

S. gallolyticus subsp. *gallolyticus* UCN34 (further designated as *S. gallolyticus*) and the genetically resembling non-pathogenic strain *S. gallolyticus* subsp. *macedonicus* CIP105685T (further designated as *S. macedonicus*) from the Pasteur collection (19, 20). *Escherichia coli* NTB5, *Salmonella typhimurium* NTB6 (16), *Staphylococcus lugdunensis* NTB8*, Enterobacter cloacae* NTB9 and *Klebsiella pneumonia* NTB10 from the Radboud strain collection. All strains were grown on Columbia blood agar or in Brain Heart Infusion (BHI) broth (Difco) supplemented with 1% glucose at 37°C/5% CO_2. *L. plantarum* was grown in de Man, Rogosa and Sharpe (MRS)-broth and *E. coli* and *E. coli Nissle* were grown in BHI at 200 rpm at 37°C/5% CO_2.

Bacterial growth experiments - To determine bacterial growth characteristics in the presence of tumor cell metabolites, CRC cell lines were first cultured for three days in standard DMEM growth medium. Next, the culture supernatants were collected (designated as spent medium) and bacterial growth in this spent medium was compared to the growth in standard medium (control condition). Every 20 minutes optical density was measured by determining the OD600 in a microplate reader (Ascent).

To determine bacterial growth rates in simulation experiments, standard DMEM medium was supplemented with the amino acids L-alanine (2 mM) or phenylalanine (2 mM). Besides these amino acids, this medium was supplemented with fructose 6-phosphate (F6P) or 3-

phosphate glyceric acid (3PG), both at a concentration of 2 mM. Combinations of F6P (1mM) and 3PG (1mM) with the amino acids L-alanine (2 mM) and phenylalanine (2 mM) were made to assess the combined effect of these substances on *S. gallolyticus* and *E. coli* growth. Media were inoculated with ~1x10^7 *S. gallolyticus* or *E. coli* and OD600 was measured every 20 minutes. Bacterial growth rates were determined at the linear part of the bacterial growth curves and plotted using Graphpad 4.0. Slope differences were determined in Graphpad 4.0 using linear regression models and considered significant at $p < 0.05$.

Protein sample collection - For 2-dimensional polyacrylamide gel electrophoresis (2D-PAGE) analysis, S. gallolyticus was grown to mid-log phase (OD600 of 0.4) in spent medium of Caco-2 or HCT116 cells. Alternatively, S. gallolyticus was grown in spent medium of Caco-2 cells in the presence of viable Caco-2 cells. As control condition S. gallolyticus was grown to mid-log phase in standard medium (OD600 of 0.2). All incubations were performed in triplicate. At the appropriate OD600, bacteria were collected (4000 g, 10 minutes) and washed 2 times with phosphate-buffered saline (PBS; 8000 g, 3 minutes). Next, bacteria were suspended in lysis solution (2mM MgCl2) containing 3 mg/ml lysozyme (Biochemica) and 100 µg/ml mutanolysin (Sigma Aldrich) and incubated at 37°C for 60 minutes. After incubation, 1% SDS was added together with a protease inhibitor cocktail (Roche). Samples were sonicated 3 times on ice at 30% with 0.3 sec intervals for 20 seconds on a DIGITAL Sonifier® UNITS Models S-250D (Branson). After sonication, benzonase (Novagen) treatment (0.625 U/µl) for 30 minutes on ice was performed to degrade remaining DNA. Insoluble material was removed by spinning the samples at 4°C for 30 minutes at 14000g. The supernatants were solubilized 1:1 in solubilization solution (7M Urea, 2M Thiourea, 10% CHAPS, 50 mM dithiotreitol (DTT) and 0.2% carrier ampholytes (pH 3-10)) and stored at -80°C until further analysis. Protein concentration in the samples was measured with the Bradford protein assay (BioRad) according to the manufacturers' instruction.

2D-PAGE - After thawing, 350 µg protein per sample was diluted in rehydration solution (final concentration: 5 mM Tris-HCl pH 8.8, 7M Urea, 3M Thiourea, 75 mM DTT, 2% carrier ampholytes (pH 3-10)). Samples were spun at 14000g for 10 minutes and the supernatant was brought onto a 17 cm IPG-strip (pH 4-7; Biorad). Strips were rehydrated overnight (o/n) with active rehydration at 50 V and 20°C. After applying moist electrode wicks, iso-electric focusing (IEF) was performed on a Biorad Protean IEF Cell using the following protocol: 1 hour at 200 V, 1 hour at 500 V, 1 hour at 1000 V, linear to 8000 V during 30 minutes, 8000V to 20.000 Vhours. Next, IPG-strips were equilibrated with equilibration solution 1 (0.375 M Tris-HCl (pH 8.8), 6 M urea, 2% SDS, 20 % glycerol, 2% DTT) for 10 minutes and subsequently with equilibration solution 2 (0.375 M Tris-HCl (pH 8.8), 6 M urea, 2% SDS, 20 % glycerol, 4% iodoacetamide) for 10 minutes. The second dimension was run on Protean II Ready gels (12% Tris-HCl; Bio-rad) in 1 xTris-Glycine electrophoresis buffer (Biorad) at 24 mA/gel during 5-6 hours using a continuous cooling system. Next, gels were fixed for 1 hour in 10% acetic acid and 50 % methanol in ddH2O. Proteins were visualized with Blue silver staining (0.12% Coommassie G-250, 10% (NH4)2·SO4, 10% H3PO4, 20% methanol). After protein staining, gels were scanned on an Odyssey gel system at 700 nm (focus offset 0.5 mm and scan intensity 4.0).

Delta-2D analysis - High-resolution TIFF files of the protein gels were loaded into Delta-2D (Decodon) and warped following the group warping strategy as outlined in the Delta-2D manual. Due to imperfect IEF, 1 gel from the condition in which S. gallolyticus was grown in spent medium from Caco-2 cells in the presence of viable Caco-2 cells was excluded from analysis. After warping, a fusion image was generated for spot detection using one of the “control” gels as master image. Spots were automatically detected by the software and visually evaluated to remove “noise” spots. Spot intensities were generated using overall normalization. For a first evaluation of the samples, scatter plots were generated. Furthermore, sample and protein expression clustering were evaluated by principal component analyses (PCA) and hierarchical clustering using complete linkage with Euclidian

distance. Statistical analysis was carried out using ANOVA for overall comparison of the groups and student's t-test (based on permutations) was used for individual comparisons of the experimental groups to the control group. Expression differences were considered significant at a p-value below 0.01.The False Discovery Rate (FDR) was set at 10 proteins or less. Spots were selected for spot identification based on statistical tests, a fold-change of at least 2 and a normalized expression value of at least 0.05 (Figure 1).

Global metabolic pathway analysis - To obtain a global picture of the affected metabolic pathways of S. gallolyticus in all three spent media conditions, significantly changed proteins that were identified in the 2D gel analysis (120 proteins, Figure 1) were mapped to the KEGG global map of metabolic pathways (21) via orthologous groups (COGs, see Supplementary Table S4) using the Signature web server (22). These pathways were visualized on the global metabolic map using iPath (23), where the color represents the average fold-change in expression of all proteins mapped to a specific pathway. A more detailed outline of the affected cellular functions was obtained by using the annotations provided by the RAST server (24), which assigns each function to a subsystem (see Supplementary Table S4). Both annotations in KEGG and RAST were used to obtain a general overview of the affected metabolic pathways.

vMaldi-MS/MS protein identification - Preparative 2D-PAA gels were prepared as described above. Protein spots were excised with a clean scalpel in a laminar flow hood to reduce keratin pollution and stored in a microtiter plate. Spots were dehydrated with acetonitrile and stored in -80 until further analysis. Next, gel-pieces were thawed and subjected to in-gel trypsin digesting as described previously (25). After digestion, peptides were extracted by sonication in a water bath for 15-20 seconds, concentrated using a centrifugal evaporator, and diluted 1:1 with 2% trifluoroacetic acid (TFA). Next, samples were spotted on a stainless steel MALDI plate. Sample analysis was performed on a linear ion trap fitted with an intermediate pressure matrix-assisted laser-desorption ionization source (vMALDI-LTQ;

Thermo Fisher Scientific) (26). In total, 5 full MS runs were analyzed, each resulting in a selection of the 10 highest peaks that were further analyzed by collision-induced dissociation fragmentation analysis. Generated RAW-data files, were analyzed with SEQUEST (Ver. 28 Rev.12) and identifications were considered significant with a peptide probability > 1e-002, and a protein probability > 1e-003. The following modifications were allowed in the search: carbamidomethylation of cysteines (fixed), oxidation of methionine (variable) and deamidation of asparagine and glutamine (variable). See supplementary Table S1 for further details on vMALDI-MS/MS protein identification, data analysis settings and validation criteria.

^{1}H-NMR-spectroscopy – Biological duplicates of media and spent media samples of Caco-2 and HCT116 with or without *S. gallolyticus* were deproteinized using Sartorius Centrisart I filters (cut-off 10 kDa; Sartorius AG, Goettingen, Germany). Before use, the filter was washed twice by centrifugation of water to remove glycerol. A small volume (20 µL) of 20.2mM trimethylsilyl-2,2,3,3-tetradeuteropropionic acid (TSP, sodium salt; Aldrich) in D_2O was added to 700 µL of the ultrafiltrate, providing a chemical shift reference (0.00 ppm) and a deuterium lock signal. Finally, 650 µL of the sample was placed in a 5mm NMR tube (Wilmad Royal Imperial; Wilmad LabGlass, USA).

Single pulse ^{1}H-NMR spectra (500 MHz) were obtained on a Bruker DMX-500 spectrometer as described by Engelke *et al*. (27). Phase and baseline were corrected manually.

All spectra were scaled to TSP and metabolite signals were fitted semi-automatically with a Lorentzian line shape. Metabolite concentrations in the spent media were calculated relative to the known concentration in the standard medium and correspondingly expressed as mM or mg/ml. The concentration of lactate in the standard medium was calculated by comparing the area of lactate with the area of the valine doublet at 1.04 ppm.

RESULTS

Growth advantage of *S. gallolyticus* in spent medium of colorectal cancer cells

To investigate the influence of CRC metabolites on the growth of *S. gallolyticus* and other intestinal bacterial strains, bacteria were inoculated in spent medium from Caco-2 cells. As indicated in Figure 2, the bacterial growth rate of *S. gallolyticus* and *S. macedonicus* in this medium was significantly increased compared to the growth rate in control medium with a factor 3.1 and 13.9 respectively ($p < 0.001$). Conversely, the growth rates of *L. plantarum*, *E. coli*, *S. lugdunensis* ($p < 0.01$), and *S. typhimurium* (not significant) were reduced in spent medium of Caco-2 cells. Similar effects on growth were observed when these bacteria were grown in spent medium from other CRC cell lines (HT-29, SW480 and HCT116; Figure S1). Together, these results suggest that cancer cell metabolism can specifically provide *S. gallolyticus* and the closely related bacterium *S. macedonicus* with a growth advantage. Since *S. macedonicus* lacks the virulence factors to become a human pathogen (16), further experiments focused on *S. gallolyticus*.

Proteome profiling of *S. gallolyticus* cells grown in spent medium from tumor cells

To investigate which metabolic pathways were enriched in *S. gallolyticus* while growing in spent media, the changes in the *S. gallolyticus* proteome were explored by 2D-PAGE analysis in the two media with the most pronounced effects, namely HCT116 and Caco-2 (see Figure S2 for original 2D-gels). To this purpose, *S. gallolyticus* responses upon incubation in spent medium from HCT116 cells, and in spent medium from Caco-2 cells in the absence or presence of viable Caco-2 cells, were compared to the control condition in which *S. gallolyticus* was grown in standard medium. The condition with viable Caco-2 cells was included to allow cross-talk within this hybrid co-culture system. A total of 665 proteins were detected with 2D-proteome analysis (Figure S3). Global analysis of these proteomes with both hierarchical clustering (Figure 3A) and principal component analysis (PCA; Figure 3B) showed that the proteomes of the replicate conditions cluster together. This indicates

that the biological replicates yielded highly similar and reproducible expression profiles, but that distinct protein spots were induced under the different experimental conditions. The expression profiles of *S. gallolyticus* grown in spent medium of Caco-2 cells were similar to the condition where also viable Caco-2 cells were present, which implies that components that were already present in the spent medium dominated the altered expression of *S. gallolyticus* proteins. The protein expression profile of *S. gallolyticus* grown in spent medium of HCT116 cells showed a somewhat different pattern than the two Caco-2 conditions (Figure 3A and B). Overall comparison with ANOVA and the individual comparisons with students t-tests of the experimental conditions with the control resulted in a total of 87 differentially expressed protein spots ($p<0.01$). An additional 89 proteins were selected for identification based upon a fold change of more than 2 ($p<0.05$) (Figure 1).

Identification of differentially expressed proteins

As indicated above, a total of 176 protein spots from the master gel were selected for in-gel tryptic digestion and peptide sequencing by vMALDI-MS/MS. Subsequent SEQUEST searches resulted in the identification of 120 protein spots (68%) (see Table S2 for annotated profiles and Table S3 for peptide hits per identified spot with probability scores). These 120 identified protein spots consisted of 78 unique proteins (Figure 1, Table 1). Thus, as depicted in Table 1, several proteins were detected in more than one protein spot. This is most likely due to post-translational protein processing such as glycosylation, phosphorylation and/or proteolytical processing. Since it is difficult to make a functional distinction between the observed isoforms, we have chosen to present an average fold change per identified protein (Table 1). Functional classification of these proteins shows that most proteins have a function in metabolism, especially in carbohydrate metabolism, amino acid metabolism and metabolism of nucleotides (Table 1). Other identified proteins are involved in protein synthesis, cell wall synthesis and cellular processes. A total of 14 proteins could not be functionally annotated. Overall, the protein expression differences of *S. gallolyticus* when this bacterium was grown in HCT116 and Caco-2 spent media compared to the control condition

pointed in the same direction. Only 6 of the 78 unique *S. gallolyticus* proteins showed opposite expression patterns in HCT116 medium compared to Caco-2 medium (indicated with an asterisk in Table 1). Thus, while hierarchical clustering and PCA of all 665 proteins suggested differential expression patterns when *S. gallolyticus* was grown in Caco-2 or HCT-116 medium, investigation of only the 176 *S. gallolyticus* proteins with significantly altered expression levels showed similar protein expression changes. This suggests that the consistent growth advantage of *S. gallolyticus* in both media conditions is most likely mediated by the same metabolic factors.

Pathway analysis reveals up-regulation of glycolysis

To visualize whether significantly altered proteins of *S. gallolyticus* in both HCT116 and Caco-2 media belonged to common pathways, the average fold changes were subjected to pathway analysis (Figure 1, Supplementary Table S4). Pathway analysis with both KEGG (Supplementary Figure S4) and RAST annotation tools indicated similar changes in bacterial metabolism when grown in Caco-2 or HCT116 medium (Table 2), although the overall changes were more pronounced in spent medium from Caco-2 cells. Most of the identified proteins belonged to the glycolysis (up-regulated) and purine metabolism pathways (down-regulated) (Table 2A and B) and showed similar outcomes when either one of the annotation tools was used. The average fold changes in the glycerolipid, glycolysis and fructose utilization pathways suggest that increased utilization of glucose and glucose derivates is a central event in *S. gallolyticus* cells grown in spent medium from both Caco-2 and HCT116 cells. A closer look, combining RAST and KEGG annotation, reveals that the glycolysis pathway was upregulated between the enzymes glucose-6-phosphate (G6P) and glyceraldehyde-3-phosphate (3PG) in both Caco-2 (Figure 4A) and HCT116 (Figure 4B) medium. However, conversion of 3PG to glycerate1-3-phosphate (G13P) was increased in Caco-2 medium and decreased in HCT116 medium, whereas the conversion of G13P to glycerate-3-phosphate was increased in HCT116 medium alone. Taken together, these findings suggest that *S. gallolyticus* preferentially forages on glucose and its break-down

products, and that these secondary glucose metabolites of tumor cells provide *S. gallolyticus* with improved growth characteristics. It should be noted that the observed changes in metabolic pathways are not just the simple result of the increased growth rate of *S. gallolyticus* but of a different employment of its preferred metabolic pathways, as shown by the fact that several pathways, such as purine metabolism, have also been down-regulated under the spent medium conditions (Table 2).

Metabolome analysis confirms up-regulation of glycolysis

To further investigate which tumor cell metabolites in spent medium could be responsible for the growth advantage of *S. gallolyticus*, the metabolites in standard medium (control) and spent medium from Caco-2 and HCT116 cells were analyzed by ^{1}H-NMR-spectroscopy before and after incubation with *S. gallolyticus* (Figure 5). Duplicate analyses were highly reproducible and indicated that both Caco-2 and HCT116 cells had a high glucose metabolism as indicated by i) the reduction of glucose (box in Figure 5 A-C) and pyruvate, and ii) an increase in lactate levels in spent medium compared to standard medium (Figure 5 A-C; Table 3). In addition, *S. gallolyticus* had an increased ability to metabolize glucose in both Caco-2 and HCT116 spent medium (Figure 5 D-F), which was shown by a reduction in glucose level of 31% in both spent media compared to 7.5 % in standard medium (Table 3). That notion that glycolysis in *S. gallolyticus* was upregulated when grown in these tumor cell media was confirmed by the increased production of pyruvate under these conditions (0% in standard medium, versus 14.7% in Caco-2 and 34.6% in HCT116; Figure 5 K-L). It must be noted, however, that intermediate glucose metabolites, such as G6P, fructose-6-phosphate (F6P) and 3PG could not be discriminated by ^{1}H-NMR spectroscopy. Therefore, the increased utilization of glucose in spent media could as well be attributed to these glucose metabolites as indicated by pathway analysis of the *S. gallolyticus* proteins with significantly altered expression levels (Figure 4). Furthermore, alanine was found to have increased levels in spent medium of both Caco-2 and HCT116 cells, whereas the alanine levels decreased after growth of *S. gallolyticus* by 30% in these media (Figure 5 G-L, Table 3),

suggesting that alanine might also be a growth factor for *S. gallolyticus.* The levels of acetoin (Figure 5 J-L), a bacterial metabolite of pyruvate metabolism, nicely reflect the increase of the bacterial glycolysis pathway in the spent media, and could therefore be used as a surrogate marker for increased glucose and glucose derivate consumption under these conditions. Taken together, pathway and ^{1}H-NMR-analysis both indicate that the glycolytic activity of *S. gallolyticus* is increased in spent medium from tumor cells.

Increased growth of *S. gallolyticus* in the presence of glucose intermediates and alanine

Finally, we investigated whether glucose derivates and the amino acids alanine and phenylalanine specifically stimulate the growth of *S. gallolyticus.* The growth of *S. gallolyticus* (advantage) and *E. coli* (disadvantage) in standard medium was compared to that in standard medium supplemented with the amino acids alanine and phenylalanine, and/or the glycolyse intermediates F6P and 3PG. As shown in Figure 6A, the growth rates of both *S. gallolyticus* and *E. coli* were significantly increased with factors 1.7 and 1.4, respectively, in medium supplemented with 2 mM F6P. However, when 2 mM 3PG was supplemented, only *S. gallolyticus* had a significant growth advantage (factor 1.6). The addition of either alanine or phenylalanine alone had no effect on the growth rate of *S. gallolyticus* (Figure 6C; control). However, in combination with 1 mM F6P or 3PG, the addition of alanine increased the growth rate of *S. gallolyticus* with a factor of about 1.4, whereas this was not observed for *E. coli* (Figure 6B and C). Taken together, these simulation experiments show that *S. gallolyticus* can specifically utilize the secondary glucose metabolites F6P and 3PG, and the amino acid alanine to increase its growth rate, which is in-line with the proteomic and metabolomic findings of this study. Furthermore, these data provide proof-of-concept for a model in which tumor cell metabolites provide a competitive advantage to a subset of the intestinal bacterial population.

DISCUSSION

The association between *S. gallolyticus* and malignancy of the intestinal tract has long been recognized, however, the underlying mechanisms still need to be resolved. Here we show for the first time that CRC cell metabolites can provide this bacterium with a specific growth advantage. Proteome and metabolome analyses point towards the increased utilization of glucose and its metabolites together with the amino acid alanine by *S. gallolyticus*, suggesting that these CRC metabolites are of particular importance for the observed growth advantage. It can be envisaged that this phenomenon may be one of the molecular mechanisms that supports the high incidence of *S. gallolyticus* infections in CRC patients (16, 28). Below, we will speculate how such a mechanism could have its place in the complex ecosystem of the gut.

The colonic lumen is a highly competitive environment, in which a balanced microbial composition is maintained at a rather stable level. The current state-of-the-literature suggests that *S. gallolyticus* is a bad colonizer of the healthy colon, whereas it has recently been shown that about 47% of the distal small intestinal (ileum) microbiota consists of Streptococci. In the ileum, where high levels of carbohydrates and dietary nutrients are available (29, 30), carbohydrate fermentation by *Streptococci* leads to the formation of lactate. Adaptation to this carbohydrate-rich environment is reflected by the enrichment for genes encoding functions in substrate transport and carbohydrate metabolism in the *S. gallolyticus* genome (19). In line with this observation, *S. bovis* strains were shown to be among the most efficient glucose fermenting bacteria in an experimental human *in vitro* gut fermentation model (TIM-2; (31)).

It seems plausible that *S. gallolyticus* cells that are shed from the ileum and enter the colonic lumen are gradually outcompeted by the colonic microbiota and disappear below the

detection level. This is reflected by the relative low fecal carriage of about 10%, and colonic mucosal colonization of 2% in the healthy human population (12, 32). However, the CRC microenvironment has some interesting similarities with the nutritional status of the ileum. Recent metabolome studies have shown that CRC tissues are associated with increased levels of lactate, glucose derivates, amino acids, lipids and fatty acids (17, 33-35). Our current *in vitro* metabolome analysis of CRC cell supernatants were in-line with these *in vivo* data and strongly suggest that the metabolic changes in the surrounding of tumor cells result in increased glucose metabolism and shedding of amino acids, which might attract glucose fermenting bacteria, such as *S. gallolyticus* that are not normally present in the colon. This could explain the fact that both fecal carriage and colonic mucosal colonization of *S. gallolyticus* in CRC patients was found to be strongly increased, to respectively 50% and 48% (12, 32). Recent deep pyrosequencing studies of 16S rRNA amplicons derived from CRC tissue biopsies and adjacent non-malignant mucosa showed that colonic malignancies did indeed strongly affect the local composition of mucosa-associated microbiota, and resulted in an increased abundance of *Fusobacteria*, *Streptococceae* and *Coriobacteria* (8, 36-38).

Although the evidence for increased glycolysis and amino acid metabolism appears to be strong, it cannot be excluded that we have missed certain metabolic features with our proteomics-based pathway analysis. First of all, not all protein spots could be identified with vMALDI-MS/MS (68% identified) and secondly not all identified proteins could be functionally annotated using KEGG (41%) or RAST (77%). Despite these limitations, both annotation systems showed similar pathway alterations and both proteome and metabolome analysis pointed in the direction of increased glucose and glucose metabolite utilization in spent media of cancer cells. Unfortunately, the direct measurement of these glucose metabolites with NMR-spectrosocopy was not possible and therefore it remains to be determined why *S. gallolyticus* is not able to use glucose as a source in standard medium, while it is more efficiently used in spent media of cancer cells or when F6P and 3PG are

added to standard medium. Future studies should be aimed at fractionation of spent media from CRC cells to identify the factors that increase the growth rate of *S. gallolyticus*. Such a biochemical approach is needed to further increase our insight in the competitive growth advantage of certain bacteria in a CRC microenvironment.

Taken together, we have shown that tumor cell metabolites that accumulate in a simulated tumor cell environment can selectively favor the growth of *S. gallolyticus*. The full impact of such tumor-associated metabolic changes on *S. gallolyticus* within a colonic microbiota should be further investigated by *in vitro* gut systems or *in vivo* models that include the ecological complexity of the gastro-intestinal tract. Ultimately, this knowledge may provide leads for novel microbiome-related tools for early detection of CRC, which is one of the major issues in human health care. Furthermore, understanding the cross-talk between CRC tumors and the intestinal microbiota may provide leads towards novel therapies or strategies to detect this disease at an early stage.

ACKNOWLEDGEMENTS

We wish to thank Angelina Goudswaard, Angela van Diepen, Hans Wessels, Lambert Lambooy, Christin Lebing and Julian Marchesi for stimulating discussions and technical support. AB was supported by the Dutch Cancer Society (KWF; project KUN 2006-3591); BED was supported by the Dutch Organization for Scientific Research (NWO; Veni grant 016.111.075); RR was supported in part by the Dutch Digestive Disease Foundation (MDLS; project WO 10-53). The funders had no role in study design, data collection and analysis, decision to publish, or preparation of the manuscript. The authors declare that they have no conflict of interest.

REFERENCES

1. Eckburg, P. B., Bik, E. M., Bernstein, C. N., Purdom, E., Dethlefsen, L., Sargent, M., Gill, S. R., Nelson, K. E., and Relman, D. A. (2005) Diversity of the human intestinal microbial flora. *Science* 308, 1635-1638

2. Hooper, L. V., Midtvedt, T., and Gordon, J. I. (2002) How host-microbial interactions shape the nutrient environment of the mammalian intestine. *Annu Rev Nutr* 22, 283-307

3. Vollaard, E. J., and Clasener, H. A. (1994) Colonization resistance. *Antimicrob Agents Chemother* 38, 409-414

4. Jemal, A., Siegel, R., Ward, E., Hao, Y. P., Xu, J. Q., and Thun, M. J. (2009) Cancer Statistics, 2009. *Ca-a Cancer Journal for Clinicians* 59, 225-249

5. Johansson, M. E., Phillipson, M., Petersson, J., Velcich, A., Holm, L., and Hansson, G. C. (2008) The inner of the two Muc2 mucin-dependent mucus layers in colon is devoid of bacteria. *Proc Natl Acad Sci U S A* 105, 15064-15069

6. Soler, A. P., Miller, R. D., Laughlin, K. V., Carp, N. Z., Klurfeld, D. M., and Mullin, J. M. (1999) Increased tight junctional permeability is associated with the development of colon cancer. *Carcinogenesis* 20, 1425-1431

7. Green, G. L., Brostoff, J., Hudspith, B., Michael, M., Mylonaki, M., Rayment, N., Staines, N., Sanderson, J., Rampton, D. S., and Bruce, K. D. (2006) Molecular characterization of the bacteria adherent to human colorectal mucosa. *J Appl Microbiol* 100, 460-469

8. Marchesi, J. R., Dutilh, B. E., Hall, N., Peters, W. H., Roelofs, R., Boleij, A., and Tjalsma, H. (2011) Towards the human colorectal cancer microbiome. *PLoS One* 6, e20447

9. Aksoy, N., and Akinci, O. F. (2004) Mucin macromolecules in normal, adenomatous, and carcinomatous colon: evidence for the neotransformation. *Macromol Biosci* 4, 483-496

10. Stecher, B., and Hardt, W. D. (2008) The role of microbiota in infectious disease. *Trends Microbiol* 16, 107-114

11. Boleij, A., and Tjalsma, H. (2012) Gut bacteria in health and disease: a survey on the interface between intestinal microbiology and colorectal cancer. *Biological reviews of the Cambridge Philosophical Society*

12. Klein, R. S., Recco, R. A., Catalano, M. T., Edberg, S. C., Casey, J. I., and Steigbigel, N. H. (1977) Association of Streptococcus bovis with carcinoma of the colon. *N Engl J Med* 297, 800-802

13. Boleij, A., van Gelder, M. M., Swinkels, D. W., and Tjalsma, H. (2011) Clinical Importance of Streptococcus gallolyticus Infection Among Colorectal Cancer Patients: Systematic Review and Meta-analysis. *Clin Infect Dis* 53, 870-878

14. Corredoira, J. C., Alonso, M. P., Garcia, J. F., Casariego, E., Coira, A., Rodriguez, A., Pita, J., Louzao, C., Pombo, B., Lopez, M. J., and Varela, J. (2005) Clinical characteristics and significance of Streptococcus salivarius bacteremia and Streptococcus bovis bacteremia: a prospective 16-year study. *Eur J Clin Microbiol Infect Dis* 24, 250-255

15. Lieberman, D. A., Weiss, D. G., Bond, J. H., Ahnen, D. J., Garewal, H., and Chejfec, G. (2000) Use of colonoscopy to screen asymptomatic adults for colorectal cancer. Veterans Affairs Cooperative Study Group 380. *The New England journal of medicine* 343, 162-168

16. Boleij, A., Muytjens, C. M., Bukhari, S. I., Cayet, N., Glaser, P., Hermans, P. W., Swinkels, D. W., Bolhuis, A., and Tjalsma, H. (2011) Novel clues on the specific association of Streptococcus gallolyticus subsp gallolyticus with colorectal cancer. *J Infect Dis* 203, 1101-1109

17. Hirayama, A., Kami, K., Sugimoto, M., Sugawara, M., Toki, N., Onozuka, H., Kinoshita, T., Saito, N., Ochiai, A., Tomita, M., Esumi, H., and Soga, T. (2009) Quantitative metabolome profiling of colon and stomach cancer microenvironment by capillary electrophoresis time-of-flight mass spectrometry. *Cancer research* 69, 4918-4925

18. Kleerebezem, M., Boekhorst, J., van Kranenburg, R., Molenaar, D., Kuipers, O. P., Leer, R., Tarchini, R., Peters, S. A., Sandbrink, H. M., Fiers, M. W., Stiekema, W., Lankhorst, R. M., Bron, P. A., Hoffer, S. M., Groot, M. N., Kerkhoven, R., de Vries, M., Ursing, B., de

Vos, W. M., and Siezen, R. J. (2003) Complete genome sequence of Lactobacillus plantarum WCFS1. *Proc Natl Acad Sci U S A* 100, 1990-1995

19. Rusniok, C., Couve, E., Da Cunha, V., El Gana, R., Zidane, N., Bouchier, C., Poyart, C., Leclercq, R., Trieu-Cuot, P., and Glaser, P. (2010) Genome sequence of Streptococcus gallolyticus: insights into its adaptation to the bovine rumen and its ability to cause endocarditis. *J Bacteriol* 192, 2266-2276

20. Schlegel, L., Grimont, F., Ageron, E., Grimont, P. A., and Bouvet, A. (2003) Reappraisal of the taxonomy of the Streptococcus bovis/Streptococcus equinus complex and related species: description of Streptococcus gallolyticus subsp. gallolyticus subsp. nov., S. gallolyticus subsp. macedonicus subsp. nov. and S. gallolyticus subsp. pasteurianus subsp. nov. *Int J Syst Evol Microbiol* 53, 631-645

21. Kanehisa, M., Araki, M., Goto, S., Hattori, M., Hirakawa, M., Itoh, M., Katayama, T., Kawashima, S., Okuda, S., Tokimatsu, T., and Yamanishi, Y. (2008) KEGG for linking genomes to life and the environment. *Nucleic acids research* 36, D480-484

22. Dutilh, B. E., He, Y., Hekkelman, M. L., and Huynen, M. A. (2008) Signature, a web server for taxonomic characterization of sequence samples using signature genes. *Nucleic acids research* 36, W470-474

23. Letunic, I., Yamada, T., Kanehisa, M., and Bork, P. (2008) iPath: interactive exploration of biochemical pathways and networks. *Trends in biochemical sciences* 33, 101-103

24. Aziz, R. K., Bartels, D., Best, A. A., DeJongh, M., Disz, T., Edwards, R. A., Formsma, K., Gerdes, S., Glass, E. M., Kubal, M., Meyer, F., Olsen, G. J., Olson, R., Osterman, A. L., Overbeek, R. A., McNeil, L. K., Paarmann, D., Paczian, T., Parrello, B., Pusch, G. D., Reich, C., Stevens, R., Vassieva, O., Vonstein, V., Wilke, A., and Zagnitko, O. (2008) The RAST Server: rapid annotations using subsystems technology. *BMC genomics* 9, 75

25. Ettwig, K. F., Butler, M. K., Le Paslier, D., Pelletier, E., Mangenot, S., Kuypers, M. M., Schreiber, F., Dutilh, B. E., Zedelius, J., de Beer, D., Gloerich, J., Wessels, H. J., van Alen, T., Luesken, F., Wu, M. L., van de Pas-Schoonen, K. T., Op den Camp, H. J., Janssen-Megens, E. M., Francoijs, K. J., Stunnenberg, H., Weissenbach, J., Jetten, M. S., and Strous,

M. (2010) Nitrite-driven anaerobic methane oxidation by oxygenic bacteria. *Nature* 464, 543-548

26. Guillard, M., Gloerich, J., Wessels, H. J., Morava, E., Wevers, R. A., and Lefeber, D. J. (2009) Automated measurement of permethylated serum N-glycans by MALDI-linear ion trap mass spectrometry. *Carbohydrate research* 344, 1550-1557

27. Engelke, U. F., Kremer, B., Kluijtmans, L. A., van der Graaf, M., Morava, E., Loupatty, F. J., Wanders, R. J., Moskau, D., Loss, S., van den Bergh, E., and Wevers, R. A. (2006) NMR spectroscopic studies on the late onset form of 3-methylglutaconic aciduria type I and other defects in leucine metabolism. *NMR in biomedicine* 19, 271-278

28. Boleij, A., Roelofs, R., Schaeps, R. M., Schulin, T., Glaser, P., Swinkels, D. W., Kato, I., and Tjalsma, H. (2010) Increased exposure to bacterial antigen RpL7/L12 in early stage colorectal cancer patients. *Cancer* 116, 4014-4022

29. Booijink, C. C., El-Aidy, S., Rajilic-Stojanovic, M., Heilig, H. G., Troost, F. J., Smidt, H., Kleerebezem, M., De Vos, W. M., and Zoetendal, E. G. (2010) High temporal and inter-individual variation detected in the human ileal microbiota. *Environmental microbiology* 12, 3213-3227

30. van den Bogert, B., de Vos, W. M., Zoetendal, E. G., and Kleerebezem, M. (2011) Microarray analysis and barcoded pyrosequencing provide consistent microbial profiles depending on the source of human intestinal samples. *Applied and environmental microbiology* 77, 2071-2080

31. Egert, M., de Graaf, A. A., Maathuis, A., de Waard, P., Plugge, C. M., Smidt, H., Deutz, N. E., Dijkema, C., de Vos, W. M., and Venema, K. (2007) Identification of glucose-fermenting bacteria present in an in vitro model of the human intestine by RNA-stable isotope probing. *FEMS Microbiol Ecol*, 126-135

32. Abdulamir, A. S., Hafidh, R. R., and Abu Bakar, F. (2010) Molecular detection, quantification, and isolation of Streptococcus gallolyticus bacteria colonizing colorectal tumors: inflammation-driven potential of carcinogenesis via IL-1, COX-2, and IL-8. *Mol Cancer* 9, 249

33. Chan, E. C., Koh, P. K., Mal, M., Cheah, P. Y., Eu, K. W., Backshall, A., Cavill, R., Nicholson, J. K., and Keun, H. C. (2009) Metabolic profiling of human colorectal cancer using high-resolution magic angle spinning nuclear magnetic resonance (HR-MAS NMR) spectroscopy and gas chromatography mass spectrometry (GC/MS). *Journal of proteome research* 8, 352-361

34. Bi, X., Lin, Q., Foo, T. W., Joshi, S., You, T., Shen, H. M., Ong, C. N., Cheah, P. Y., Eu, K. W., and Hew, C. L. (2006) Proteomic analysis of colorectal cancer reveals alterations in metabolic pathways: mechanism of tumorigenesis. *Mol Cell Proteomics* 5, 1119-1130

35. Righi, V., Durante, C., Cocchi, M., Calabrese, C., Di Febo, G., Lecce, F., Pisi, A., Tugnoli, V., Mucci, A., and Schenetti, L. (2009) Discrimination of healthy and neoplastic human colon tissues by ex vivo HR-MAS NMR spectroscopy and chemometric analyses. *J Proteome Res* 8, 1859-1869

36. Castellarin, M., Warren, R. L., Freeman, J. D., Dreolini, L., Krzywinski, M., Strauss, J., Barnes, R., Watson, P., Allen-Vercoe, E., Moore, R. A., and Holt, R. A. (2012) Fusobacterium nucleatum infection is prevalent in human colorectal carcinoma. *Genome Res* 22, 299-306

37. Kostic, A. D., Gevers, D., Pedamallu, C. S., Michaud, M., Duke, F., Earl, A. M., Ojesina, A. I., Jung, J., Bass, A. J., Tabernero, J., Baselga, J., Liu, C., Shivdasani, R. A., Ogino, S., Birren, B. W., Huttenhower, C., Garrett, W. S., and Meyerson, M. (2012) Genomic analysis identifies association of Fusobacterium with colorectal carcinoma. *Genome Res* 22, 292-298

38. Tjalsma, H., Boleij, A., Marchesi, J. R., and Dutilh, B. E. (2012) A Bacterial Driver-Passenger Model for Colorectal Cancer: Beyond the Usual Suspects. *Nature Reviews Microbiology* accepted for publication

FIGURE LEGENDS

FIG1. Flow-diagram of protein and pathway analysis

A total of 665 proteins was identified with 2D-PAGE analysis. Based on statistical analysis with ANOVA and t-tests a total 87 differentially expressed protein spots ($p<0.01$) and an additional 89 protein spots with a fold change of more than 2 ($p<0.05$) were selected for identification. By in-gel tryptic digestion, vMALDI-MS/MS peptide sequencing and subsequent SEQUEST protein database searches, a total of 120 protein spots could be identified resulting in a total of 78 unique identified proteins. The expression values of these 78 unique proteins were subjected to pathway analysis; average fold changes were used when a protein was found in multiple spots. A total of 71 proteins could be mapped to orthologous groups and of these proteins 32 mapped to the KEGG database, whereas 60 of the 78 proteins could be directly mapped to the RAST database in an alternative pathway annotation strategy.

FIG 2. Bacterial growth in spent medium of Caco-2 cells

Bacterial growth rates were determined by linear regression analysis of the linear part of the growth curves as shown for *S. gallolyticus* (A), *S. macedonicus* (B), *L. plantarum* (C), *E. coli* (D), *S. lugdunensis* (E), and *S. typhimurium* (F). Growth rates were significantly increased in spent medium from Caco-2 (green lines) as compared to standard medium (control; red lines) for *S. gallolyticus* and *S. macedonicus* ($p < 0.001$). Conversely, the growth rates of *S. lugdunensis, L. plantarum* and *E. coli* were significantly higher in standard medium as compared to spent medium from Caco-2 cells ($p < 0.01$), whereas no different growth rates were observed for *S. typhimurium*. These results suggest that *S. gallolyticus* and *S. macedonicus* can forage on excreted Caco-2 cell metabolites, whereas this is not the case for other intestinal bacteria.

FIG 3. Hierarchical clustering and principal component analysis

Protein expression levels of *S. gallolyticus* grown in standard medium (A), spent medium of Caco-2 cells (B) or HCT116 cells (C), or in spent medium of Caco-2 cells in the presence of viable Caco-2 cells (D) were visualized using hierarchical clustering analysis (panel A) and principal component analysis (panel B); numbers refer to the biological replicas of each experimental condition. Both these analyses showed that the replicate experiments of each condition clustered together. Furthermore, the two independent Caco-2 conditions, with and without viable cells, (B and D) had similar expression patterns.

FIG 4. Proteomic changes in the glycolysis pathway

Differentially expressed proteins were mapped to the KEGG global map of metabolic pathways via orthologous groups and to annotated with RAST (COGs, see Supplementary Table S4). The proteins that were up and down-regulated in the glycolysis pathway with both methods combined are shown for Caco-2 (A) and HCT116 (B). The glycolytic pathway was increased from glucose 6-phophate to 3-phophate glyceric acid for both HCT116 and Caco-2 eventually leading to the production of pyruvate (A and B). Average fold change > 1 (*red*), average fold change <-1 (*green*),average fold change between +1 and -1 (*grey*).

FIG 5. ^{1}H-NMR-profiles of Caco-2, HCT116 and *S. gallolyticus* metabolites

500 MHz ^{1}H-NMR spectra (10 – 0.5 ppm) of standard medium before (A) and after (D) growth of *S. gallolyticus* and spent medium of Caco-2 and HCT116 cells before (B and C) and after (E and F) growth of *S. gallolyticus*. Spectra G-L show an expanded scale for the 0.8 – 2.55 ppm region of the respective A-F spectra. The corresponding concentrations of several of these metabolites are indicated in Table 3. Assigned peaks: Lactic acid (LA), glucose (box in A-F), valine (VAL), leucine (LEU), isoleucine (ILEU), acetoine (AT), alanine (ALA), lysine (LYS), acetic acid (A), pyruvic acid (P) and succinic acid (S).

FIG 6. Effect of F6P, 3PG, alanine and phenylalanine on the growth of *S. gallolyticus* and *E. coli*

(A) The growth rates of *S. gallolyticus* and *E. coli* in standard medium (control, *black*), were compared to those in standard medium supplemented with 2 mM fructose-6-phosphate (F6P, *dark-grey*) and 2 mM glycerate-3-phosphate (3PG, *light-grey*). The effect of alanine (*dark-grey*) or phenylalanine (*light-grey*) supplementation on the growth rates of *E. coli* and *S. gallolyticus* in standard medium with or without 1 mM F6P or 3PG is shown in panels B and C, respectively. Calculation of the growth rates was based on 3 independent experiments. Bars represent the ratio between the growth rate in supplemented medium to that in standard medium. Evaluation with linear regression analysis was used to define if the growth rates were significantly different from each other. Significant differences ($p < 0.05$) are indicated with an asterisk (*).

Table 1. Identified *S. gallolyticus* proteins with significant changes in expression

spot nr	functional category[1]	GALLO-code	protein	Caco-2[2]	HCT116[2]	v-Caco-2[2]
Cell envelope and cellular processes						
1, 2	1.7	GALLO_0608	cell division initiation protein DivIVA	-4.20		-3.61
3	1.2	GALLO_2047	manganese ABC transporter, substrate-binding liprotein and adhesin	-2.52	-4.11	
4, 67	1.4	GALLO_0211	NADPH-dependent FMN reductase	1.48	1.82	2.09
5, 6	1.2	GALLO_1412	ABC transporter, substrate-binding protein	1.30	2.91	
7	1.1	GALLO_0830	dTDP 4-keto 6-deoxyglucose 3,5-epimerase	1.59	1.28	1.35
64	1.2	GALLO_1555	amino acid ABC transporter, ATP-binding protein	-1.67	-2.36	
65	1.1	GALLO_0829	Glucose-1-phosphate thymidylyltransferase		-2.14	
66	1.4	GALLO_0791	F0F1 ATP synthase alpha chain			-3.15
Intermediary metabolism						
8, 10, 16, 18	2.3	GALLO_0028	phosphoribosylaminoimidazole synthetase	-4.56	-2.78	-3.57
9	2.1	GALLO_1129	lactate dehydrogenase	-5.41	-6.09	
11	2.3	GALLO_2088	Deoxy UTP pyrophosphatase (dUTPase)	-3.25	-8.30	-4.92
12	2.3	GALLO_0025	phosphoribosylaminoimidazole succinocarboxamide synthetase	-3.05	-1.23	-2.97
13, 26, 89	2.1	GALLO_1458	enolase	-0.10	0.58	0.01
14	2.1	GALLO_1137	deoxyribose-phosphate aldolase	-2.63	-1.35	-2.24
15, 20, 22	2.1	GALLO_0255	fructose-bisphosphate aldolase	-0.24	1.72	0.40
17, 19, 30, 74, 78, 86	2.1	GALLO_1996	glyceraldehyde-3-phosphate dehydrogenase	2.65	-2.87	2.09
21	2.4	GALLO_0337	dioxygenases related to 2-nitropropane dioxygenase	1.55	1.72	1.53
23	2.1	GALLO_1995	phosphoglycerate kinase		6.24	
24	2.2	GALLO_1744	phosphoglycerate dehydrogenase	2.24	2.68	
25	2.2	GALLO_1293	glutamate dehydrogenase	2.37	2.27	
27, 76	2.3	GALLO_1766	uracil phosphoribosyltransferase	1.71	1.53	1.33
28, 69, 88	2.1	GALLO_0990	Pyruvate kinsase	-0.35	-2.62	0.12
29	2.3	GALLO_0968	orotidine 5'-phosphate decarboxylase	6.20	5.29	7.42
31	2.4	GALLO_0023	putative fatty acid/phospholipid synthesis protein PlsX	12.23		
68	2.3	GALLO_0970	orotate phosphoribosyltransferase	-2.81	-1.78	-2.04
70	2.3	GALLO_0034	phosphoribosylaminoimidazole carboxylase I	-2.35	-2.26	
71	2.3	GALLO_0032	phosphoribosylglycinamide synthetase	-2.29	-1.77	-2.83
72	2.3	GALLO_0037	adenylosuccinate lyase	-2.19	-2.67	
73	2.1	GALLO_0698	oxidoreductase, aldo/keto reductase family	-2.05	-2.26	-2.21
75	2.2	GALLO_1038	serine hydroxymethyltransferase	-1.72		-3.38
77	2.3	GALLO_2134	adenylosuccinate synthase	-1.36	-1.90	-2.18
80	2.3	GALLO_1025	guanosine 5'-monophosphate oxidoreductase	-1.22	1.86	-2.05
81	2.2	GALLO_0151	glutamyl aminopeptidase			-2.56
82	2.3	GALLO_0639	dihydroorotate dehydrogenase (catalytic subunit)		2.01	
83	2.2	GALLO_0307	alpha-keto-beta-hydroxylacil reductoisomerase		2.17	
84	2.1	GALLO_1318	fructose 1-phosphate kinase			2.15
85	2.3	GALLO_0705	ribonucleoside-diphosphate reductase (major subunit)			3.28
87	2.1	GALLO_2098	glucose-6-phosphate isomerase	1.67	2.26	
90	2.4	GALLO_0333	enoyl-CoA hydratase	2.24		
91	2.1	GALLO_0746	Nadp Dependent Aldehyde Dehydrogenase	2.25		
92	2.2	GALLO_1353	Chorismate synthase	2.29	1.52	
93	2.2	GALLO_0931	Xaa-His dipeptidase	2.53		2.55
Information pathways						
32, 36, 96	3.7	GALLO_1912	ribosomal protein S6	-3.59	-1.83	-3.30
33	3.7	GALLO_1140	ribosomal protein subunit S20	-3.79	-1.99	-3.88
34, 37, 47, 48, 49, 97, 99, 101, 103, 105, 106	3.7	GALLO_1511	translation elongation factor Tu	11.81	1.43	3.39
35	3.7	GALLO_0064	ribosomal protein S8		-2.10	-9.48
38	3.5	GALLO_0646	transcriptional regulator	-1.87		-2.23
39, 42, 45	3.7	GALLO_1479	ribosomal protein L19	1.27	0.98	0.11
40	3.7	GALLO_0219	ribosomal protein S15	-1.19		2.30
41	3.7	GALLO_1640	ribosome recycling factor		-5.38	
43	3.5	GALLO_1815	transcription elongation factor	1.68	1.47	2.01
44	3.7	GALLO_1998	ribosomal protein S7	3.12	1.85	2.22
46	3.5	GALLO_1319	transcriptional regulator, DeoR family	6.53	3.51	
94, 95	3.7	GALLO_1997	translation elongation factor G	-2.22	-2.60	-3.11
98	3.7	GALLO_0491	methionyl-tRNA formyltransferase			3.76
100	3.7	GALLO_0981	30S ribosomal protein S1 homolog	1.85	2.08	
102	3.7	GALLO_0082	tyrosyl-tRNA synthetase	2.13		
104	3.7	GALLO_0251	trigger factor (prolyl isomerase)	2.31	-2.51	
Other functions						
50	4.2	GALLO_0592	peroxide resistance protein Dpr	-6.60	-2.61	-5.05
51	4.3	GALLO_0432	hypothetical protein	9.62		8.75
107	4.1	GALLO_2161	heat shock protein, chaperonin, 33 kDa	-2.71		-3.78
108	4.2	GALLO_0662	superoxide dismutase	-2.04	-1.18	-1.56
109, 110, 111	4.1	GALLO_0243	heat shock protein 70, chaperone protein DnaK	-0.35	-0.59	-0.09
112	4.2	GALLO_0418	thioredoxin reductase	3.58		5.50
Similar to unknown proteins						
52, 56, 59, 63, 113, 120	5.2	GALLO_1879	hypothetical protein	1.94	0.96	-0.54
53, 54	5.2	GALLO_2228	hypothetical protein	-9.06	-4.45	-8.63
55	5.2	GALLO_1955	hypothetical protein	-5.99	-2.33	-3.60
57	5.2	GALLO_1714	hypothetical protein			-7.14
58, 60	5.2	GALLO_1295	hypothetical protein	4.37	1.75	3.54
60	5.2	GALLO_1295	hypothetical protein			
61,62	5.2	GALLO_1805	hypothetical protein	15.39		39.90
79	5.2	GALLO_2168	hypothetical protein	-1.22	2.01	-1.55
114	5.2	GALLO_0605	hypothetical protein	-2.53	-1.21	-1.92
115	5.2	GALLO_2223	hypothetical protein	-2.30		
116	5.2	GALLO_2108	hypothetical protein	-2.29	-1.62	-1.77
117	5.2	GALLO_2188	hypothetical protein	-1.53	-2.18	
118	5.2	GALLO_0604	hypothetical protein		3.14	2.30
119	5.2	GALLO_1788	hypothetical protein	2.45		2.69

[1] **functional categories: 1.1 Cell Wall; 1.2 Transport/binding proteins and lipoproteins; 1.4 Membrane bioenergetics; 1.7 Cell division; 2.1 Metabolism of carbohydrates and related molecules; 2.2 Metabolism of amino acids and related molecules; 2.3 Metabolism of nucleotides and nucleic acids; 2.4 Metabolism of lipids; 3.5 RNA synthesis; 3.7 Protein synthesis; 3.9 protein folding; 4.1 Adaptation to atypical functions; 4.2 detoxification; 4.3 antibiotic production; 5.2 From other organisms; 5.3 from Streptococcus**

[2] **Fold changes of the specified condition compared to the control condition with a p-value <0.05. Fold changes of proteins that have been identified in more than 1 protein spot are presented as an average fold change. NOTE: proteins can be detected in more than one spot due to protein phosphorylation, glycosylation and/or proteolytical processing. Since all of these isoforms may contribute to protein function, we have chosen to present an average fold-change for each unique protein.**

*** Proteins that have opposite expression in Caco-2 medium versus HCT-116 medium**

v-Caco-2 = *S. gallolyticus* grown in medium of Caco-2 cells in the presence of viable Caco-2 cells

Table 2. Global pathway analysis of significantly altered protein expression patterns

KEGG Pathway	# PROTEINS (up/down) Caco-2	# PROTEINS (up/down) HCT116	AVERAGE FC Caco-2	AVERAGE FC HCT116
Alanine, aspartate and glutamate metabolism	2 (2/0)	2 (2/0)	2.31	1.71
Glycerolipid metabolism	3 (2/1)	3 (2/1)	4.14	0.38
Glycolysis/Gluconeogenesis	15 (8/7)	15 (9/6)	0.72	0.56
Purine metabolism	12 (2/10)	12 (3/9)	-1.73	-1.26
Pyrimidine metabolism	5 (2/3)	5 (3/2)	0.32	-0.24
Starch and sucrose metabolism	1 (0/1)	1 (0/1)	-1.16	-1.27
Valine, leucine and isoleucine biosynthesis	4 (4/0)	4 (3/1)	2.04	0.77
Vitamine B6 metabolism	7 (3/4)	7 (3/4)	0.7	-0.46
Bile acid biosynthesis	4 (3/1)	4 (3/1)	0.68	0.53
Butyrate metabolism	5 (4/1)	5 (4/1)	0.87	1.09

RAST annotation	# PROTEINS (up/down) Caco-2	# PROTEINS (up/down) HCT116	AVERAGE FC Caco-2	AVERAGE FC HCT116
Fatty acid biosynthesis	2 (2/0)	2 (2/0)	1.90	1.53
Fructose utilization	2 (2/0)	2 (2/0)	3.88	2.29
Vitamin B6 Biosynthesis	8 (4/4)	8 (4/4)	0.84	0.38
Bacterial cell division	6 (3/3)	6 (2/4)	-0.95	-0.10
Amino acid biosynthesis	4 (3/1)	4 (3/1)	1.12	1.31
Purine biosynthesis	10 (0/10)	10 (1/9)	-2.74	-1.91
Pyrimidine synthesis	4 (2/2)	4 (3/1)	1.48	1.66
Glycolysis/Gluconeogenesis	19 (11/8)	19 (13/6)	0.76	0.70

Table 3. Metabolic profiles of standard and spent medium of Caco-2 and HCT116 cells

	Valine*	Alanine*	Tyrosine*	Phenyl-alanine*	Glucose**	Pyruvate**	Lactate*	Acetoin[1]
chemical shift	*1.04*	*1.48*	*6.9*	*7.34*	*5.24*	*2.38*	*1.33*	*1.38*
without bacteria								
Standard medium[2]	0.8	0.1	0.4	0.4	4.5	110	1.61	0
	100%	*100%*	*100%*	*100%*	*100%*	*100%*	*100%*	
Caco-2 spent medium	0.73	0.2	0.4	0.41	3.9	29.5	8.4	0
	91.3%	*200.0%*	*100.0%*	*102.5%*	*86.7%*	*26.8%*	*521.7%*	
HCT116 spent medium	0.5	0.12	0.29	0.3	1.4	16	31.7	0
	62.5%	*120.0%*	*72.5%*	*75.0%*	*31.1%*	*14.5%*	*1968.9%*	
after growth of *S. gallolyticus*								
Standard medium	0.78	0.09	0.4	0.4	4.2	110	4.97	4
	97.5%	*90.0%*	*100.0%*	*100.0%*	*93.3%*	*100.0%*	*308.7%*	
Caco-2 spent medium	0.66	0.17	0.37	0.37	2.5	45.6	22.06	20
	82.5%	*170.0%*	*92.5%*	*92.5%*	*55.6%*	*41.5%*	*1370.2%*	
HCT116 spent medium	0.4	0.09	0.27	0.27	0	54	44.5	22
	50.0%	*90.0%*	*67.5%*	*67.5%*	*0.0%*	*49.1%*	*2764.0%*	

*mM, **mg/L

[1]the production of acetoin is expressed as an arbitrary unit compared to internal control TSP (see Materials and Methods)

[2]Standard medium concentrations were used as reference values for calculation of concentrations and percentages

FIG. 1 Flow-diagram of protein and pathway analysis

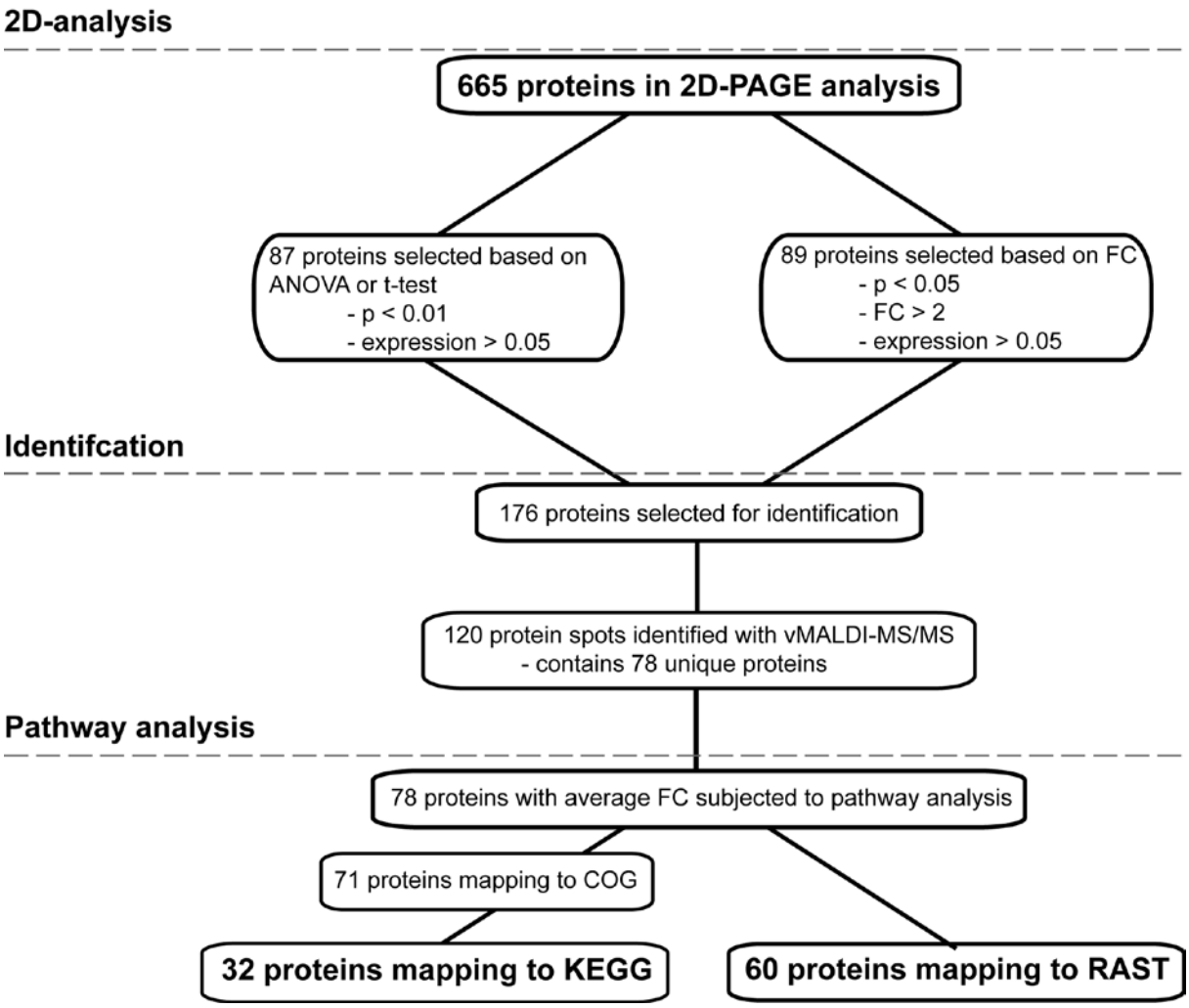

FIG. 2 Bacterial growth in spent medium of Caco-2 cells

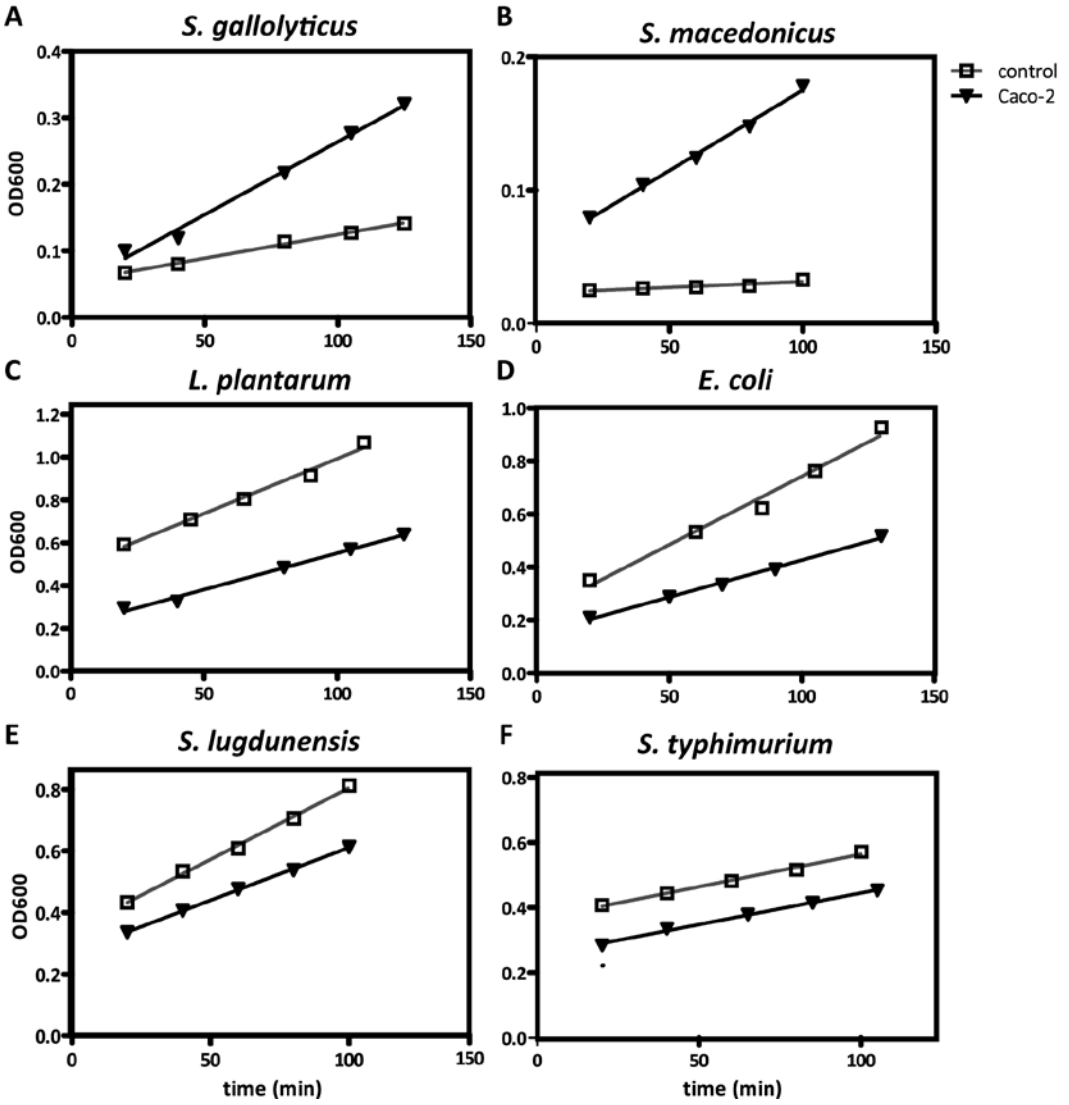

FIG 3. Hierarchical clustering and principal component analysis

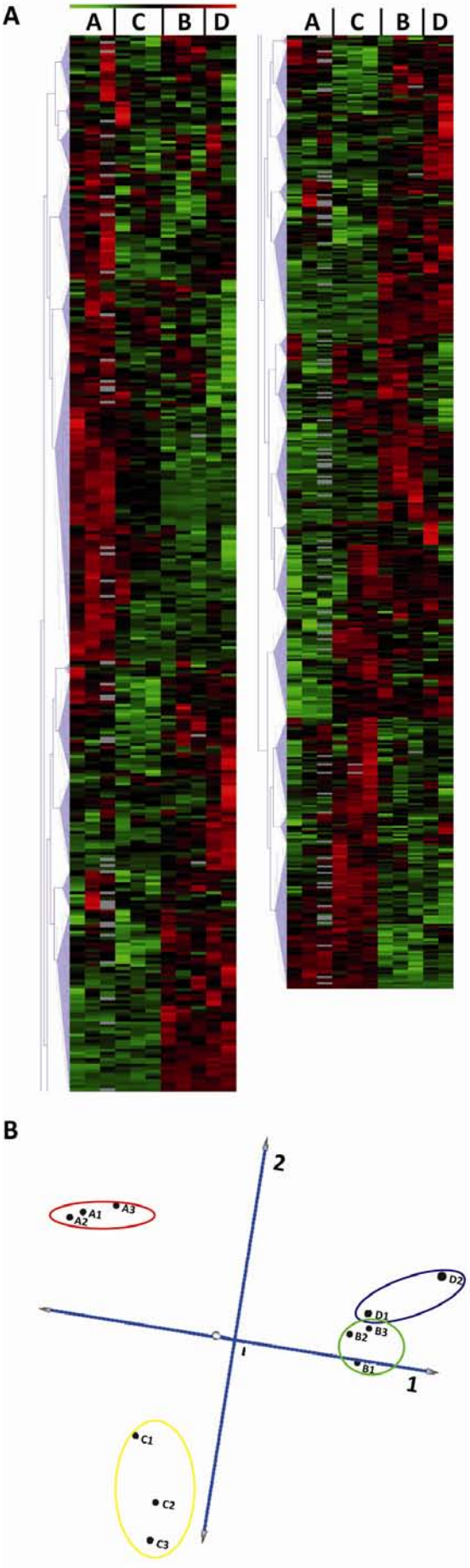

FIG. 4 Proteomic changes in the glycolysis pathway

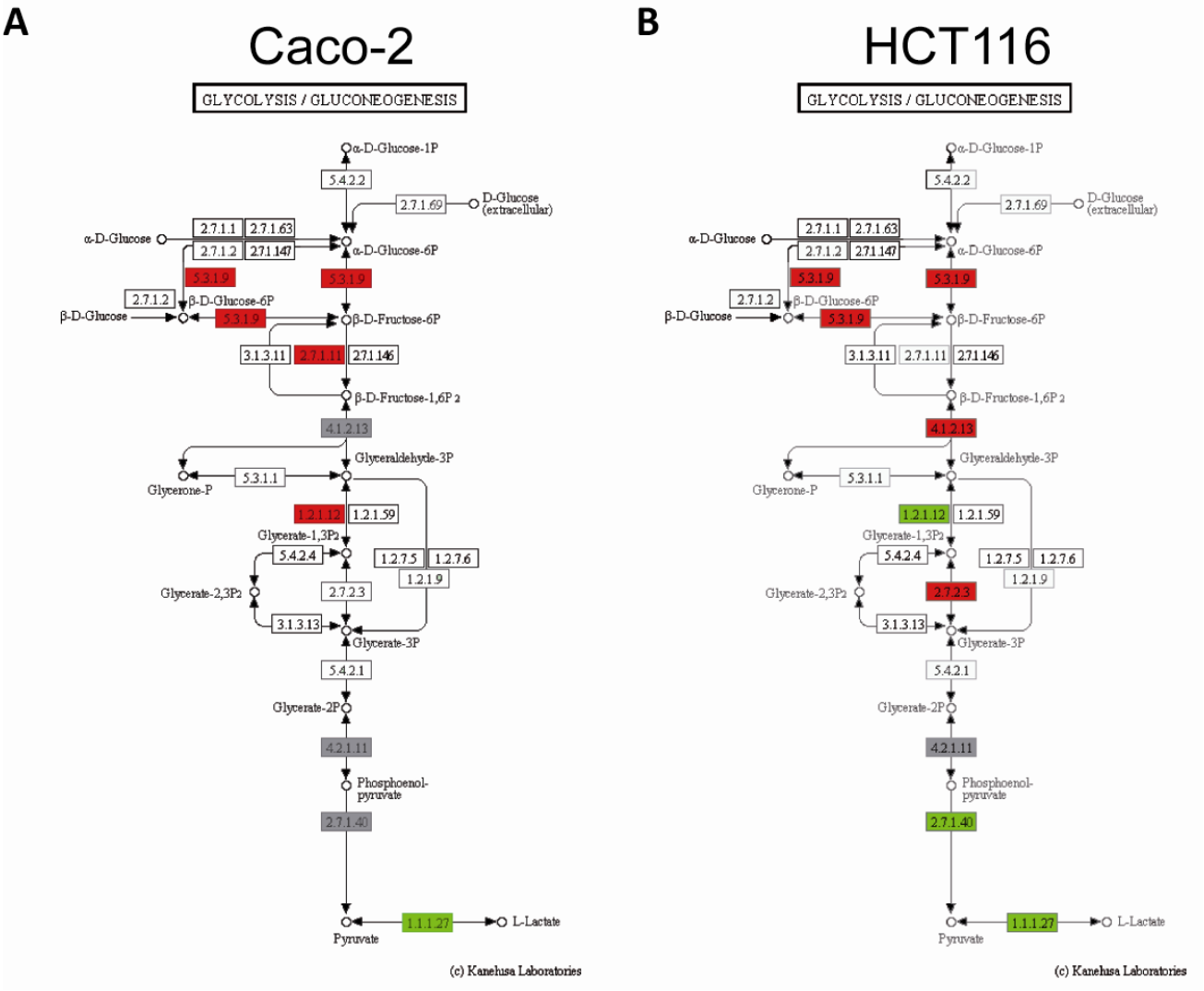

FIG. 5 ^{1}H-NMR profiles ofCaco-2, HCT116 and *S. gallolyticus* metabolites

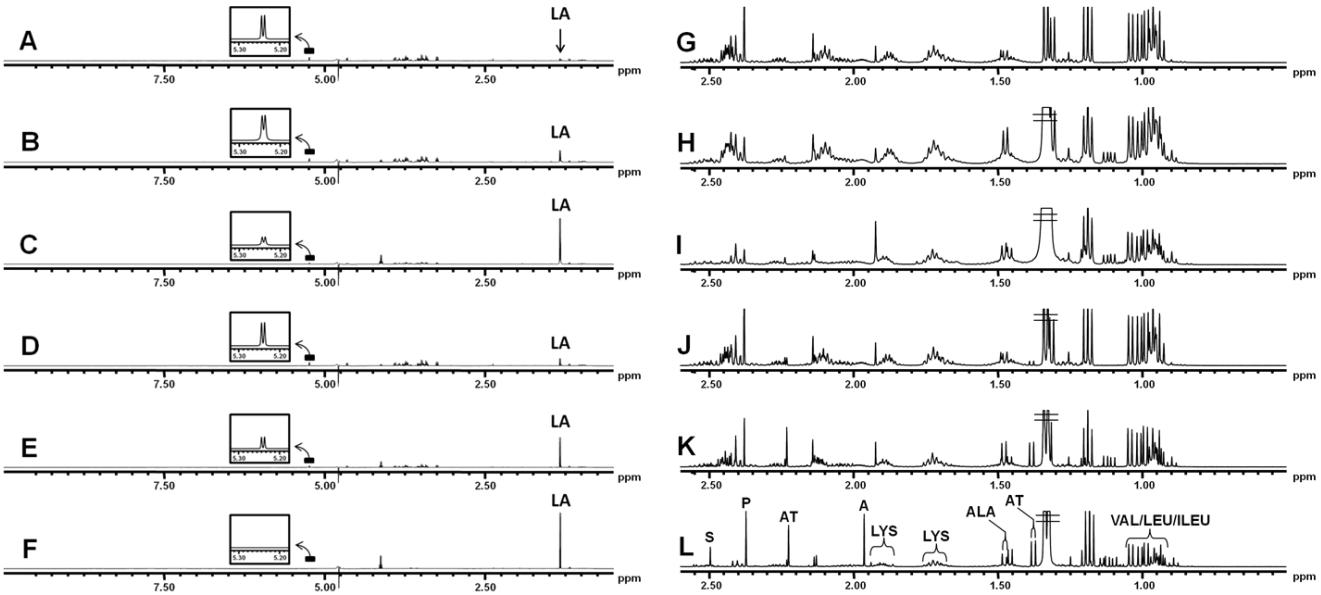

FIG. 6 Effect of F6P, 3PG, alanine and phenylalanine on the growth of *S. gallolyticus* and *E. coli*